lncRNA CASC2 inhibits lipopolysaccharide-induced acute lung injury via miR-27b/TAB2 axis

XIAOQUAN LI[1*], JINGXIN MO[2*], JUN LI[3] and YALIN CHEN[4]

[1]Critical Care Center, Shiyan People's Hospital; Departments of [2]Respiratory Intensive Care, [3]Respiratory I and [4]Respiratory II, Shiyan People's Hospital, Shiyan, Hubei 442000, P.R. China

Received December 6, 2019; Accepted September 15, 2020

DOI: 10.3892/mmr.2020.11606

Abstract. Long non-coding RNA (lncRNA) cancer susceptibility candidate 2 (CASC2) has been reported to exert an important role in acute lung injury (ALI). The present study aimed to investigate the potential underlying mechanism of CASC2 in ALI progression. Reverse transcription-quantitative PCR was conducted to examine the expression of CASC2, microRNA (miR/miRNA)-27b and TGF-β activated kinase 1 and MAP3K7-binding protein 2 (TAB2) in A549 cells. Cell viability and apoptosis were analyzed using 3-(4,5-dimethylthiazol-2-yl)-2,5-diphenyltetrazolium bromide assay and flow cytometry. Enzyme-linked immunosorbent assay was used to measure the levels of inflammatory-related cytokines to assess the inflammatory response, including interleukin-1β (IL-1β), IL-6 and tumor necrosis factor α (TNF-α). The binding sites of miR-27b in CASC2 or TAB2 were predicted using LncBase or microT-CDS software, following which dual-luciferase reporter and RNA binding protein immunoprecipitation assays were performed to confirm the target relationship between miR-27b and CASC2 or TAB2. The protein expression of TAB2 was detected by western blotting. The decreased viability, and increased apoptosis and inflammatory responses were attenuated by the accumulation of CASC2 in lipopolysaccharide (LPS)-stimulated A549 cells. CASC2 could directly bind to miR-27b in A549 cells. CASC2 protected A549 cells from LPS-triggered injury by downregulating miR-27b. TAB2 was a target of miR-27b in A549 cells. The influence of miR-27b depletion was reversed by the silencing of TAB2 in an ALI cell model. CASC2 could increase the expression of TAB2 by serving as a competing endogenous RNA of miR-27b in A549 cells. Collectively, the results suggested that CASC2 attenuated LPS-induced injury in the ALI cell model by modulating the miR-27b/TAB2 axis.

Correspondence to: Dr Jun Li, Department of Respiratory I, Shiyan People's Hospital, 39 Chaoyang Middle Road, Shiyan, Hubei 442000, P.R. China
E-mail: lkhzhd@163.com

Dr Yalin Chen, Department of Respiratory II, Shiyan People's Hospital, 39 Chaoyang Middle Road, Shiyan, Hubei 442000, P.R. China
E-mail: daqcwr@163.com

*Contributed equally

Key words: acute lung injury, lipopolysaccharide, CASC2, microRNA-27b, TGF-β activated kinase 1 and MAP3K7-binding protein 2, inflammation

Introduction

Acute lung injury (ALI) and its severe form, acute respiratory distress syndrome, are common inflammatory lung diseases with high mortality of 30-40% that are triggered by severe trauma, sepsis and pneumonia (1,2). Lipopolysaccharide (LPS) derives from the cell wall of gram-negative bacteria, and it plays a crucial role in inflammatory responses (3,4). Therefore, finding the molecules involved in the development of ALI is indispensable for the treatment of ALI.

Long non-coding RNAs (lncRNAs) are a group of non-coding RNAs (ncRNAs) with >200 nucleotides. lncRNA cancer susceptibility candidate 2 (CASC2) has been indicated as an important molecule involved in the pathogenesis of numerous types of cancer (5-8). For instance, Wang *et al* (9) reported that CASC2 prevented the epithelial-mesenchymal transition of hepatocellular carcinoma cells via microRNA (miR/miRNA)-367/F-box/WD repeat-containing protein 7 signaling. Ba *et al* (10) demonstrated that CASC2 inhibited the proliferation and motility of osteosarcoma cells via miR-181a. As for ALI, Li *et al* (11) revealed that CASC2 was downregulated in LPS-treated A549 cells, and CASC2 accumulation attenuated LPS-induced ALI *in vivo* and *in vitro*. Overall, the present study aimed to investigate the function of CASC2 in ALI, as well as its functional mechanism.

miRNAs, as another group of ncRNAs, could regulate the physiological and pathological processes by regulating the expression of target genes (12-14). miRNAs have been reported to participate in the initiation and progression of lung inflammation (15). Huang *et al* (16) demonstrated that miR-27b promoted LPS-induced ALI by regulating nuclear factor erythroid 2-related factor 2 (Nrf2) and NF-κB signaling. The present study aimed to elucidate the underlying mechanism of miR-27b in ALI.

TGF-β activated kinase 1 and MAP3K7-binding protein 2 (TAB2) serves as an important upstream adaptor

of interleukin-1 (IL-1) signaling to function. TAB2 has been reported to be involved in the pathogenesis of LPS-induced ALI (17). However, the function of TAB2 in ALI remains to be revealed.

The present study intended to uncover the role and the working mechanism of CASC2 in LPS-induced ALI cell model.

Materials and methods

Cell culture. Human alveolar epithelial adenocarcinoma cell line A549 was acquired from American Type Culture Collection. A549 cells ($2x10^5$ cells/well) in 6-well plates were grown in the Roswell Park Memorial Institute-1640 (RPMI-1640) medium (Gibco; Thermo Fisher Scientific, Inc.) containing 10% fetal bovine serum (FBS; Gibco; Thermo Fisher Scientific, Inc.), 100 U/ml penicillin and 100 μg/ml streptomycin in a humidified atmosphere at 37˚C and 5% CO_2.

LPS treatment. A549 cells were cultivated in 6-well plates ($2x10^5$ cells/well), and 1 μg/ml LPS (Sigma-Aldrich; Merck KGaA) or control [dimethyl sulfoxide (DMSO); Sigma-Aldrich; Merck KGaA] was mixed with the culture medium when the confluence reached ~80%, and the cells were incubated for 24 h according to a previous article (18).

Cell transfection. To achieve CASC2 overexpression or knockdown, CASC2 overexpression plasmid (CASC2; 1 μg), pcDNA (1 μg), small interfering RNA control (si-con; 5'-UUCUCCGAACGUGUCACGUUU-3'; 100 nM) or CASC2 specific siRNA (si-CASC2; 5'-AGACUAUAAUGAUACCUUGGG-3'; 100 nM) were transfected into A549 cells ($3x10^5$ cells/well). To achieve miR-27b overexpression or knockdown, miRNA control (miR-con; 5'-UUCUCCGAACGUGUCACGUUU-3'; 50 nM), miR-27b mimic (miR-27b; 5'-CCGAAGAUGCUCACCAGCCC-3'; 50 nM), miR-27b inhibitor (anti-miR-27b; 5'-AUGUUCUUGAAAGCCGAU-3'; 20 nM) or anti-miR-con (5'-UUGUACUACACAAAAGUACUG-3'; 20 nM) were transfected into A549 cells ($3x10^5$ cells/well). si-TAB2 (5'-ACAACUUCAGGUACUUCAGGG-3'; 100 nM) was transfected into A549 cells ($3x10^5$ cells/well) to achieve TAB2 silencing, and si-con (5'-UUCUCCGAACGUGUCACGUUU-3'; 100 nM) was used as the control. The aforementioned RNA and overexpression plasmids were purchased from Shanghai GenePharma Co., Ltd., and the transfection was carried out with Lipofectamine® 3000 (Invitrogen; Thermo Fisher Scientific, Inc.). After transfection for 24 h, transfected cells were used for subsequent analysis.

Experimental grouping. In rescue experiments of miR-27b for CASC2, A549 cells were transfected with CASC2 plasmid (1 μg) or pcDNA (1 μg) alone or together with miR-27b (50 nM) or miR-con (50 nM) for 24 h followed by 1 μg/ml LPS treatment for 24 h. Thus, A549 cells were divided into six groups: Control, LPS, LPS + pcDNA, LPS + CASC2, LPS + CASC2 + miR-con and LPS + CASC2 + miR-27b.

In rescue experiments of TAB2 for miR-27b, A549 cells were transfected with anti-miR-27b (20 nM) or anti-miR-con (20 nM) alone or together with si-TAB2 (100 nM) or si-con (100 nM) for 24 h followed by 1 μg/ml LPS treatment for 24 h. Thus, A549 cells were divided into six groups: Control, LPS, LPS + anti-miR-con, LPS + anti-miR-27b, LPS + anti-miR-27b + si-con and LPS + anti-miR-27b + si-TAB2.

Reverse transcription-quantitative PCR (RT-qPCR). Total RNA from A549 cells was extracted using TRIzol® (Beyotime Institute of Biotechnology). The reverse transcription of CASC2 and the mRNA of TAB2 was performed using BeyoRT™ First Strand cDNA Synthesis Kit (Beyotime Institute of Biotechnology) at 42˚C for 60 min, whereas the cDNA of miR-27b was obtained with One Step miRNA RT kit (HaiGene) at 37˚C for 60 min followed by 85˚C for 5 sec. U6 and glyceraldehyde-3-phosphate dehydrogenase (GAPDH) served as the internal references for miR-27b, CASC2 and TAB2. The expression of miR-27b, TAB2 and CASC2 was measured using the $2^{-\Delta\Delta Cq}$ method (19). The PCR reaction was conducted using SYBR-Green [Roche Diagnostics (Shanghai) Co., Ltd.] and an ABI 7500 thermal cycler (Applied Biosystems; Thermo Fisher Scientific, Inc.) with the following primers: CASC2 forward, 5'-GCACATTGGACGGTGTTTCC-3' and reverse, 5'-CCCAGTCCTTCACAGGTCAC-3'; miR-27b forward, 5'-AAAAGTCGACCGAAGATGCTCACCAGCCCTT-3' and reverse, 5'-AAAAGTCGACGGCAGTGGCCTCTGCCTGGC-3'; TAB2 forward, 5'-AGTACAAGATATCTTTATGG-3' and reverse, 5'-TGCTGTCTGTGGCTCCTGCT-3'); U6 forward, 5'-ATGGGTCGAAGTCGTAGCC-3' and reverse, 5'-TTCTCGGCGTCTTCTTTCTCG-3'; and GAPDH forward, 5'-ATGTTCCAGTATGACTCCACTCACG-3' and reverse, 5'-GAAGACACCAGTAGACTCCACGACA-3'.

3-(4,5-Dimethylthiazol-2-yl)-2,5-diphenyltetrazolium bromide (MTT) assay. A549 cells were plated in 96-well cell culture plates at the density of $5x10^3$ cells/well. Following LPS stimulation and relevant transfection, 20 μl 5 mg/ml MTT reagent (Sigma-Aldrich; Merck KGaA) was added into the supernatant of A549 cells. A549 cells were incubated with MTT in the incubator at 37˚C with 5% CO_2 for 4 h. The culture medium was discarded, and A549 cells were incubated with DMSO (Sigma-Aldrich; Merck KGaA) to dissolve formazan crystals. The absorbance of each well was measured at 490 nm using a microplate reader.

Cell apoptosis analysis. The adherent and non-adherent A549 cells were harvested and washed using phosphate buffered saline buffer. A549 cells ($3x10^5$ cells) were probed with Annexin V-fluorescein isothiocyanate and propidine iodide using the Apoptosis Detection Kit (BD Biosciences). A FACS CantoII flow cytometer (BD Biosciences) was used to identify the apoptotic A549 cells, and the apoptotic rate was analyzed using BD FACSDiva software (version 8.0.1; BD Biosciences). The apoptotic rate indicated the percentages of apoptotic A549 cells in the early stage (Q4) and late stage (Q2).

Enzyme-linked immunosorbent assay (ELISA). Human IL-1β (cat. no. DLB50), IL-6 (cat. no. D6050) and tumor necrosis factor α (TNF-α; cat. no. DTA00D) ELISA kits (R&D Systems, Inc.) were used to examine the concentrations of inflammatory cytokines in the supernatant of A549 cells. Briefly, A549 cells were seeded into 96-well plates ($5x10^3$ cells/well), and A549 cells were stimulated with the relevant treatment the next day. After centrifuging at 2,000 x g for 5 min at 4˚C,

cell supernatant was collected to examine the secretion of inflammatory cytokines according to the instructions of the ELISA kits.

Bioinformatics analysis. The miRNA targets of CASC2 were predicted using LncBase software v2.0 (http://carolina.imis.athena-innovation.gr/diana_tools/web/index.php?r=lncbasev2/index) from DIANA Tools, while microT-CDS software v5.0 (http://www.microrna.gr/microT-CDS) from DIANA Tools was used to predict the mRNA targets of miR-27b.

Dual-luciferase reporter assay. A dual-luciferase reporter assay was performed to explore the interaction between miR-27b and CASC2 or TAB2 in A549 cells. Transfection was performed using Lipofectamine® 3000 (Invitrogen; Thermo Fisher Scientific, Inc.). CASC2 gene sequences, including predicted wild-type (WT) or mutant-type (MUT) binding sites of miR-27b, were inserted into pmirGLO vectors (Promega Corporation). miR-con, miR-27b, anti-miR-con or anti-miR-27b and CASC2-WT or CASC2 MUT were co-transfected into A549 cells ($4x10^4$ cells/well). A Dual-Luciferase® Reporter Assay system (Promega Corporation) was utilized to measure the luciferase activity after transfection for 48 h, and the firefly luciferase activity was normalized to *Renilla* luminescence. The same protocol was used for TAB2.

RNA binding protein immunoprecipitation (RIP) assay. RNA-protein or RNA-RNA complex were isolated using Magna RIP™ RNA-Binding Protein Immunoprecipitation Kit (EMD Millipore). A549 cells ($2x10^5$ cells) were disrupted using RIP lysis buffer for 5 min on ice. The antibodies, including anti-Argonaute 2 (anti-Ago2; cat. no. MABE253; EMD Millipore) at the dilution of 1:50 and anti-Immunoglobulin G (anti-IgG; cat. no. TS-1L-BK; EMD Millipore) at the dilution of 1:100 were incubated with protein A/G beads for 1 h at 4˚C. Then, the A549 cell lysate was mixed with the beads to incubate for 4 h at 4˚C. Beads were washed twice using PBS buffer (Sangon Biotech Co., Ltd.), and the mixture was centrifuged at 21,000 x g for 10 min at 4˚C. RNA was extracted using TRIzol® (Beyotime Institute of Biotechnology), and the immunoprecipitated RNA was detected by RT-qPCR.

Western blot assay. Western cell lysis buffer (Beyotime Institute of Biotechnology) was used to disrupt A549 cells, and the proteins were quantified using a Pierce BCA Protein Assay kit (Thermo Fisher Scientific, Inc.). The quantified protein samples (25 μg) were separated on the 5% stacking and 12% separating gels, and subsequently transferred to a polyvinylidene fluoride membrane. The membrane was blocked using 5% skimmed milk for 1 h at room temperature. The membrane was incubated with anti-TAB2 at the dilution of 1:5,000 (cat. no. ab172412; Abcam) and anti-β-actin at the dilution of 1:20,000 (cat. no. ab115777; Abcam) at 4˚C overnight, followed by incubation with a horseradish peroxidase-conjugated secondary antibody (cat. no. ab205718; Abcam) at the dilution of 1:5,000 for 2 h at room temperature. Several X-ray films were used to visualize the protein signal through Pierce™ ECL Western Blotting Substrate (Thermo Fisher Scientific, Inc.). Image Lab analysis software (v4.0; Bio-Rad Laboratories, Inc.) was utilized to evaluate the intensities of protein bands.

Animal experiment. A total of 12 BALB/c mice (weight, 23-28 g; age, 8 weeks) were obtained from Experimental Animal Center of Huazhong Agricultural University (Wuhan, China) and maintained in a specific-pathogen-free environment under standard conditions of 22˚C, 60% humidity and a 12 h light/dark cycle. These nude mice were supplied food and water *ad libitum*. All experimental procedures were approved by The Ethical Committee on Animal Research of Shiyan People's Hospital (Shiyan, China) and were in accordance with guidelines provided by the National Institutes of Health Guide for the Care and Use of Laboratory Animals (20). Mice were arbitrarily divided into four groups (n=3), including the Control group (intraperitoneal injection of 30 mg/kg normal saline), LPS group (intraperitoneal injection of 30 mg/kg LPS), LPS + pcDNA group (transfection with pcDNA empty vector before LPS treatment) and LPS + CASC2 group (transfection with CASC2 before LPS treatment). Transfection was conducted using a microinjector to inject the transfection complexes (50 μl) into the trachea of the mice. After 12 h of transfection, these nude mice were euthanized using sodium pentobarbital (100 mg/kg) and the right lung (free of heart and trachea) were removed. The breathing of the mice was monitored to verify the death. No mice died during this experiment. Right lung was rinsed briefly using PBS buffer (Sangon Biotech Co., Ltd.), and then the right lung was weighed to obtain the wet weight. The right lung was baked at 56˚C for 72 h to acquire the dry weight. Wet-to-dry (W/D) ratio was obtained by dividing the wet weight of the right lung by the dry weight. The myeloperoxidase (MPO) activity of lung tissues was obtained using an MPO determination kit (Jiancheng Company; http://www.njjcbio.com/products.asp?id=354) at 460 nm. The expression of CASC2 was detected using RT-qPCR. The levels of IL-1β, IL-6 and TNF-α were measured using ELISA kits.

Statistical analysis. Statistical analysis was carried out using GraphPad Prism 7 software (GraphPad Software, Inc.). Normally distributed data are presented as the mean ± standard deviation. Comparisons between groups were analyzed using Student's t-test or one-way analysis of variance followed by Tukey's post hoc test as appropriate. $P<0.05$ was considered to indicate a statistically significant difference.

Results

CASC2 overexpression ameliorates LPS-triggered ALI. To investigate the expression pattern and biological function of CASC2 in ALI, a ALI cell model was established by treating A549 cells with 1 μg/ml LPS for 24 h. The overexpression efficiency of the CASC2 plasmid was high in A549 cells (Fig. S1A). As shown in Fig. 1A, the expression of CASC2 was decreased in the ALI cell model compared with in non-treated A549 cells. Besides, the expression of CASC2 was increased in A549 cells treated with LPS and the CASC2 overexpression plasmid. LPS stimulation reduced viability and induced apoptosis of A549 cells (Fig. 1B and C). In addition, the overexpression of CASC2 protected A549 cells against

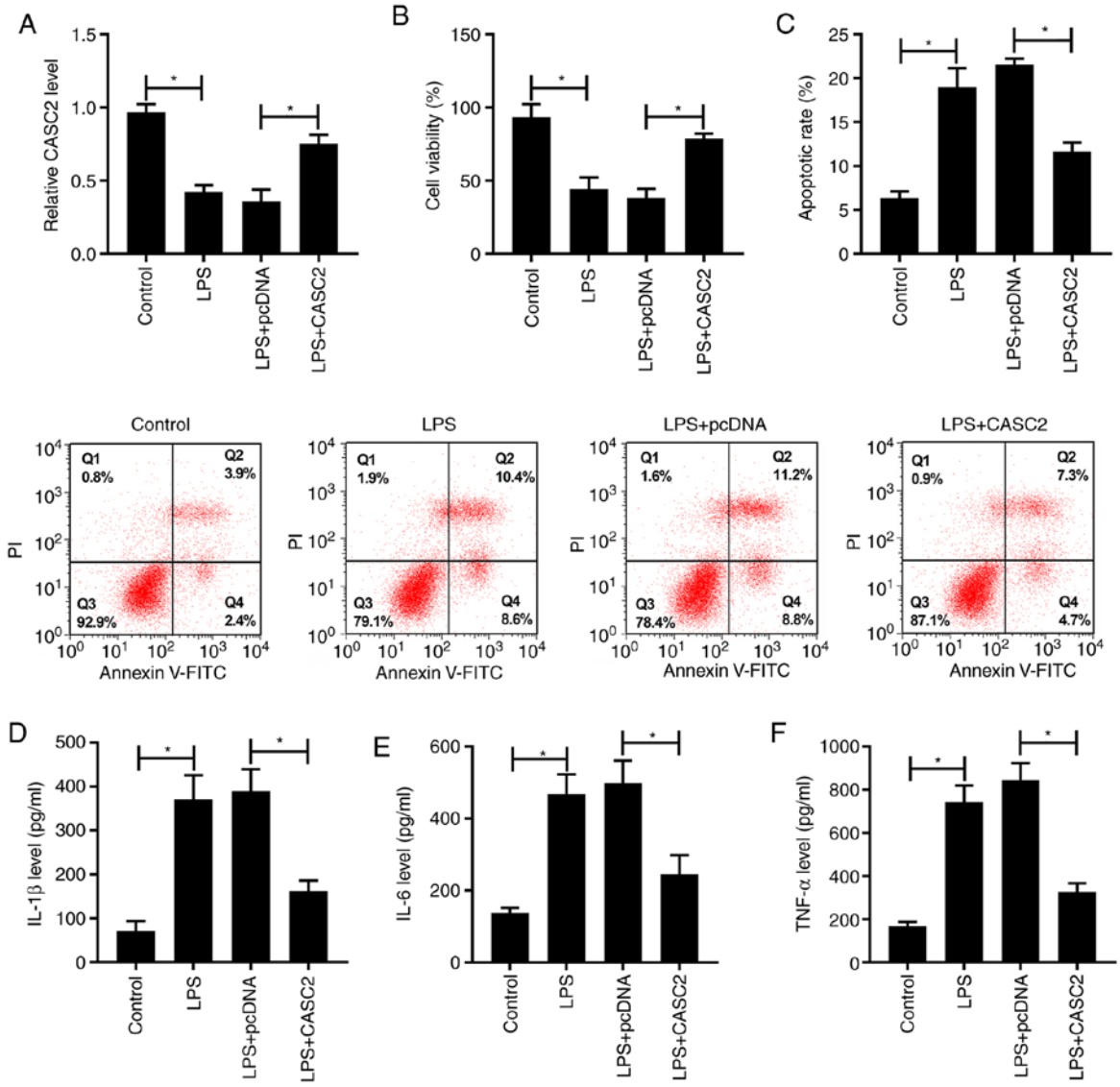

Figure 1. CASC2 overexpression ameliorates LPS-induced acute lung injury. A549 cells were stimulated with LPS, LPS + pcDNA or LPS + CASC2. (A) The expression of CASC2 was detected in A549 cells via reverse transcription-quantitative PCR. (B) A 3-(4,5-dimethylthiazol-2-yl)-2,5-diphenyltetrazolium bromide assay was performed to measure the viability of A549 cells. (C) The apoptotic rate of A549 cells was analyzed by flow cytometry. The inflammatory factors in A549 cells, including (D) IL-1β, (E) IL-6 and (F) TNF-α, were examined by ELISA. *P<0.05. CASC2, cancer susceptibility candidate 2; LPS, lipopolysaccharide; IL, interleukin; TNF-α, tumor necrosis factor α.

LPS-induced injury. The inflammatory reaction was activated in the ALI model, and the transfection of CASC2 suppressed LPS-triggered inflammation (Fig. 1D-F). In summary, these data suggested that LPS-induced ALI could be attenuated by the overexpression of CASC2.

CASC2 could directly bind to miR-27b to downregulate its expression. miR-27b was predicted to be a potential target of CASC2 using LncBase database, and the putative binding sites are listed in Fig. 2A. The transfection efficiencies of miR-27b and anti-miR-27b were high in A549 cells, as determined by RT-qPCR (Fig. S1B). The dual-luciferase reporter assay results showed that transfection of miR-27b or anti-miR-27b significantly decreased or increased the luciferase activity in the CASC2-WT group, respectively (Fig. 2B). Besides, the luciferase activity in the CASC2-MUT group remained unaffected. Furthermore, a RIP assay was conducted to detect whether CASC2 was present in RNA-induced silencing complex (RISC), and the results revealed that CASC2 and miR-27b could be detected in the RISC (Fig. 2C), suggesting that CASC2 could bind to miR-27b in A549 cells. LPS exposure could elevate the expression of miR-27b in A549 cells (Fig. 2D). The transfection of si-CASC2 significantly reduced CASC2 expression in A549 cells (Fig. S1A). CASC2 overexpression significantly downregulated the expression of miR-27b (Fig. 2E), whereas transfection with si-CASC2 significantly increased the expression of miR-27b in A549 cells, suggesting that miR-27b was inversely regulated by CASC2 in A549 cells. These data indicated that miR-27b was a target of CASC2, and CASC2 negatively regulated the expression of miR-27b in A549 cells.

CASC2 protects A549 cells against LPS-induced inflammatory damage by downregulating miR-27b. To further explore

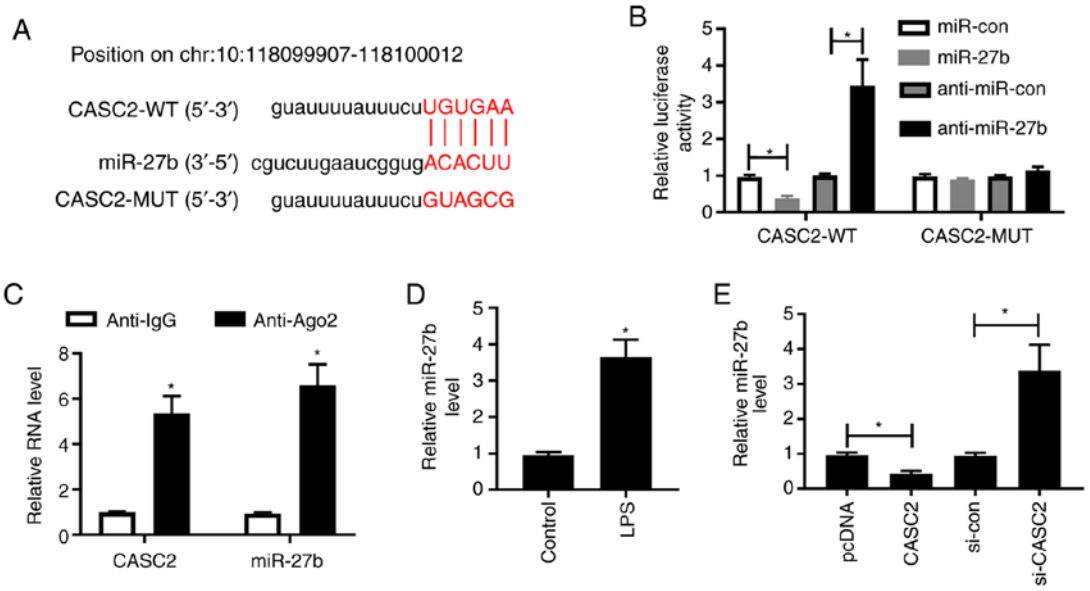

Figure 2. CASC2 could directly bind to miR-27b to downregulate its expression. (A) The miR-27b binding sequence in CASC2 was predicted using LncBase software. (B) A dual-luciferase reporter assay was performed in A549 cells co-transfected with CASC2-WT or CASC2-MUT and miR-con, miR-27b, anti-miR-con or anti-miR-27b. (C) The association between miR-27b and CASC2 was verified by performing a RNA binding protein immunoprecipitation assay. (D) RT-qPCR was conducted to measure the expression of miR-27b in A549 cells treated with LPS. (E) RT-qPCR was performed to detect the expression of miR-27b in A549 cells transfected with pcDNA, CASC2, si-con or si-CASC2. *P<0.05 vs. control group. CASC2, cancer susceptibility candidate 2; LPS, lipopolysaccharide; miR, microRNA; WT, wild-type; MUT, mutant; con, control; RT-qPCR, reverse transcription-quantitative PCR; si-, small interfering RNA; Ago2, Argonaute 2; IgG, Immunoglobulin G.

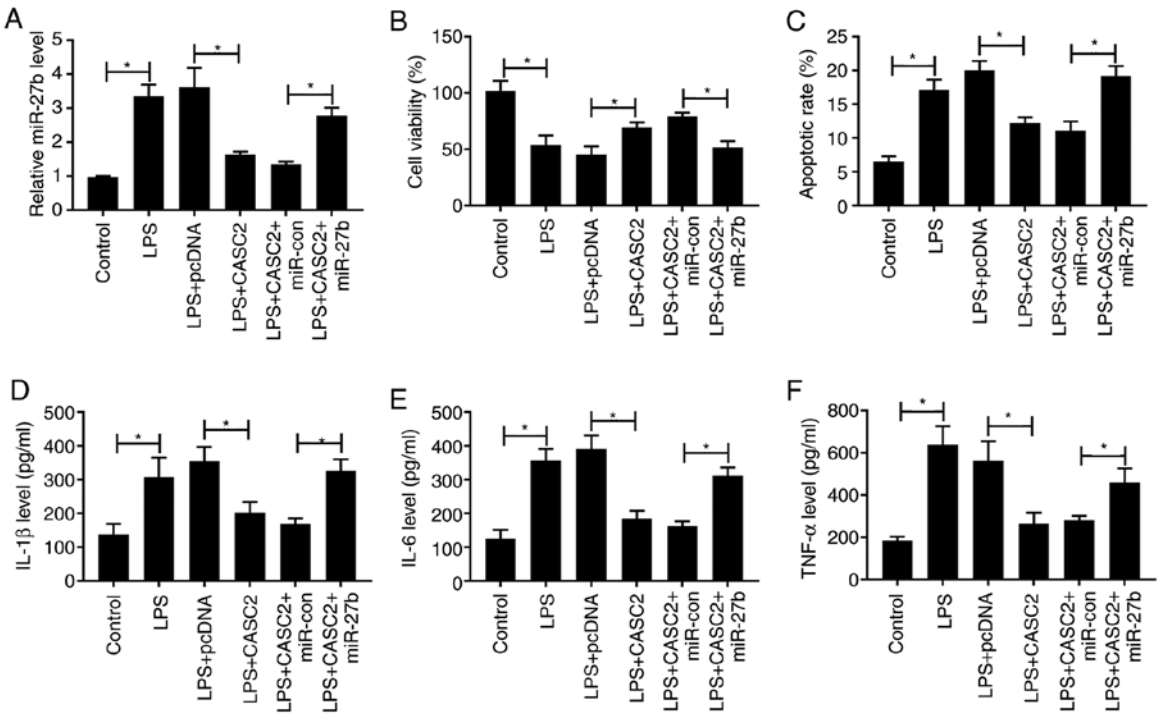

Figure 3. CASC2 protects A549 cells against LPS-induced inflammatory damage by downregulating miR-27b. A549 cells were transfected with CASC2 plasmid (1 μg) or pcDNA (1 μg) alone or together with miR-27b (50 nM) or miR-con (50 nM) for 24 h followed by 1 μg/ml LPS treatment for 24 h. (A) The expression of miR-27b was examined in A549 cells by reverse transcription-quantitative PCR. (B) The viability of A549 cells was measured using a 3-(4,5-dimethylthiazol-2-yl)-2,5-diphenyltetrazolium bromide assay. (C) Flow cytometry was conducted to detect the apoptosis of A549 cells. (D-F) ELISA was performed to examine the concentrations of inflammatory factors in the supernatant of A549 cells. *P<0.05. CASC2, cancer susceptibility candidate 2; LPS, lipopolysaccharide; IL, interleukin; TNF-α, tumor necrosis factor α; miR, microRNA; con, control.

the functions of miR-27b and CASC2 in LPS-induced ALI, A549 cells were divided into six groups: Control, LPS, LPS + pcDNA, LPS + CASC2, LPS + CASC2 + miR-con or LPS + CASC2 + miR-27b. As shown in Fig. 3A, CASC2 overexpression reduced the expression of miR-27b in the ALI cell model, whereas the expression of miR-27b was increased

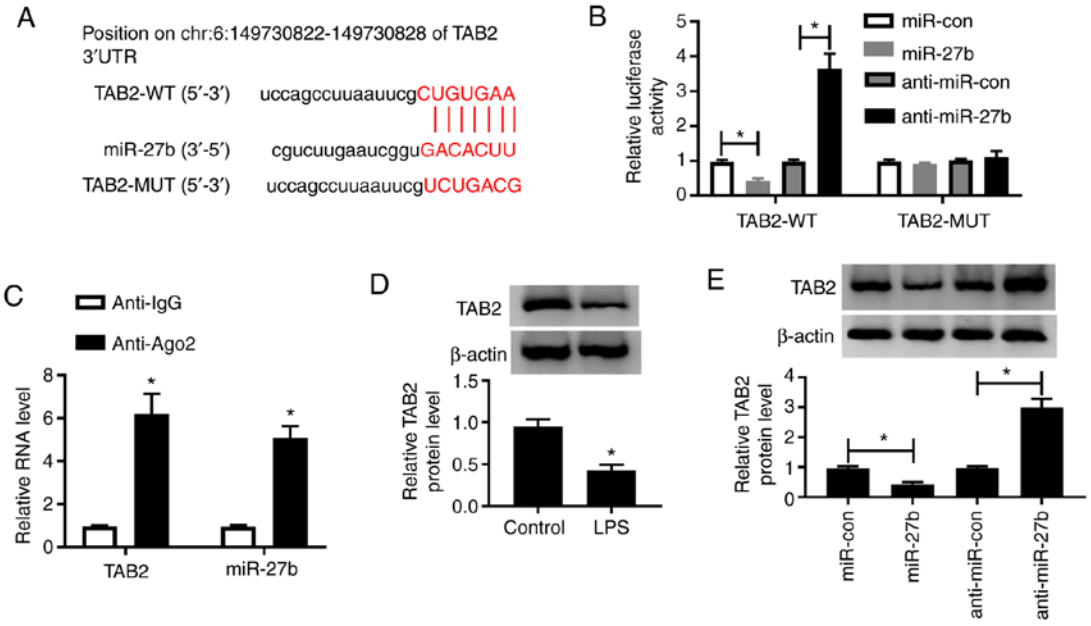

Figure 4. TAB2 is a target of miR-27b in A549 cells. (A) The binding sites of miR-27b in the 3'UTR of TAB2 were predicted using microT-CDS software. (B) The target relationship between miR-27b and TAB2 was confirmed by a dual-luciferase reporter assay. (C) A RNA binding protein immunoprecipitation assay was carried out to validate the association between miR-27b and TAB2 in A549 cells. (D) The expression of TAB2 in LPS-induced A549 cells was examined by western blotting. (E) Western blotting was conducted to measure the expression of TAB2 in A549 cells transfected with miR-con, miR-27b, anti-miR-con or anti-miR-27b. *P<0.05 vs. control group. TAB2, TGF-β activated kinase 1 and MAP3K7-binding protein 2; LPS, lipopolysaccharide; miR, microRNA; 3'UTR, 3'untranslated region; WT, wild-type; MUT, mutant; con, control; Ago2, Argonaute 2; IgG, Immunoglobulin G.

in LPS-stimulated cells co-transfected with CASC2 and miR-27b. The addition of miR-27b reversed the protective effect of CASC2 transfection on the viability of ALI model cells (Fig. 3B). Meanwhile, the apoptosis was significantly increased in the LPS + CASC2 + miR-27b group compared with that in the LPS + CASC2 + miR-con group (Fig. 3C). Subsequently, it was found that the inhibitory effect of CASC2 overexpression on the inflammatory response was reversed by the overexpression of miR-27b in ALI model cells (Fig. 3D-F). Collectively, these data suggested that CASC2 suppressed LPS-stimulated ALI by downregulating the expression of miR-27b.

TAB2 is a target of miR-27b in A549 cells. microT-CDS software was used to search the target genes of miR-27b, the putative miR-27b binding sequence in the 3'untranslated region (3'UTR) of TAB2 is shown in Fig. 4A. The luciferase activity was significantly decreased or increased in A549 cells co-transfected with TAB2-WT and miR-27b or anti-miR-27b, respectively (Fig. 4B). These results revealed that TAB2 was a direct target of miR-27b in A549 cells. To further validate these results, a RIP assay was carried out. As shown in Fig. 4C, TAB2 and miR-27b were co-precipitated with Ago2, demonstrating that TAB2 could bind to miR-27b in A549 cells. Besides, LPS treatment reduced the protein expression of TAB2 in A549 cells (Fig. 4D). A549 cells transfected with miR-con, miR-27b, anti-miR-con or anti-miR-27b were used to explore the modulatory relationship between miR-27b and TAB2. As exhibited in Fig. 4E, miR-27b transfection reduced the expression of TAB2, whereas depletion of miR-27b led to the opposite effect in A549 cells. In summary, TAB2 was shown to be a target of miR-27b in A549 cells, and miR-27b could negatively regulate the expression of TAB2.

TAB2 depletion attenuates the protective effect of miR-27b silencing on LPS-induced ALI. To determine whether TAB2 was involved in the miR-27b-mediated inflammatory injury of ALI model cells, anti-miR-27b and si-TAB2 were co-transfected into ALI model cells. The knockdown efficiency of si-TAB2 was high in A549 cells (Fig. S1C). As indicated in Fig. 5A, the expression of TAB2 was increased following the depletion of miR-27b in the ALI model, and this promotor effect was reversed by the silencing of TAB2. Besides, miR-27b depletion protected A549 cells against the LPS-induced reduction in viability, and increase in apoptosis and inflammatory-related cytokine expression. These effects were reversed by the co-transfection of si-TAB2 and anti-miR-27b (Fig. 5B-F). Taken together, miR-27b accelerated LPS-induced ALI by targeting and downregulating TAB2 expression.

CASC2 upregulates the expression of TAB2 by functioning as a competing endogenous (ce)RNA of miR-27b in A549 cells. The expression of TAB2 was elevated by the transfection of CASC2, and the addition of miR-27b decreased the expression of TAB2 in A549 cells (Fig. 6A). Furthermore, CASC2 silencing caused a significant reduction in the expression of TAB2, whereas the co-transfection of anti-miR-27b and si-CASC2 increased the expression of TAB2 in A549 cells (Fig. 6B). These data showed that TAB2 was regulated by the CASC2/miR-27b axis in A549 cells.

CASC2 overexpression attenuates LPS-triggered ALI in lung tissues. BALB/c mice were divided into the indicated four groups. Lung tissue injury was assessed by measuring the W/D ratio, MPO activity and inflammation. As presented in

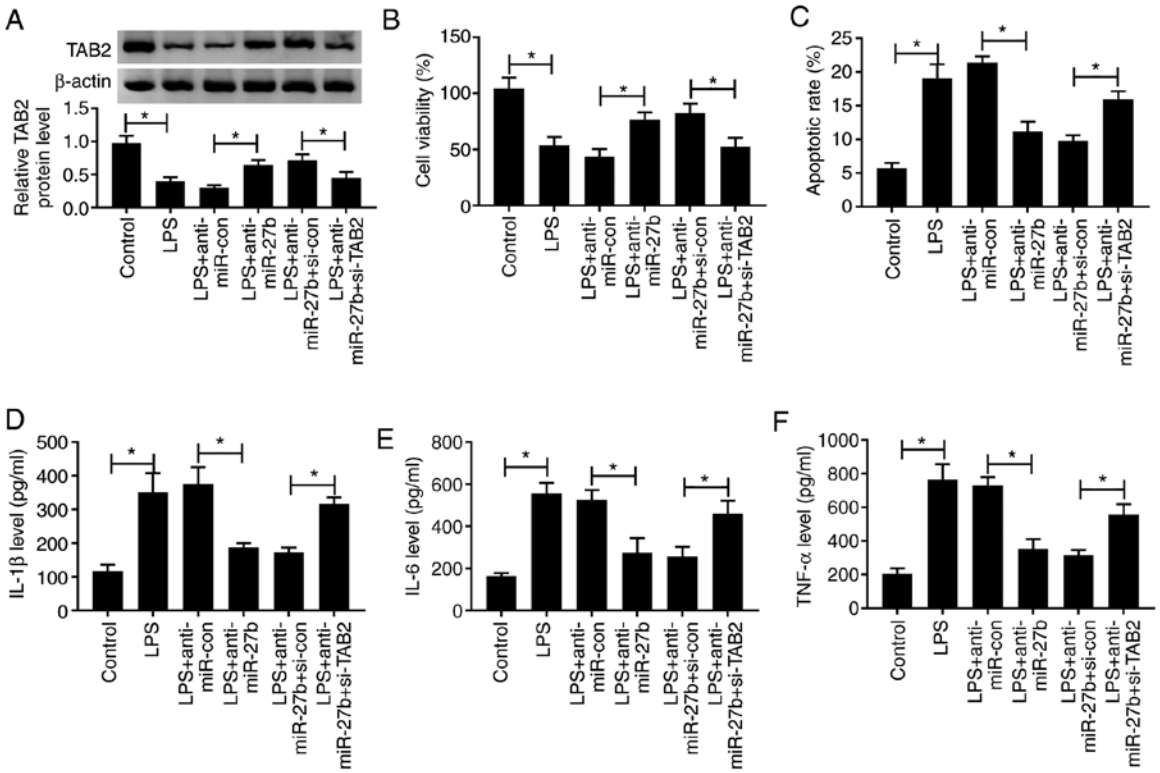

Figure 5. TAB2 knockdown attenuates the protective effect of miR-27b silencing on LPS-induced ALI. A549 cells were transfected with anti-miR-27b (20 nM) or anti-miR-con (20 nM) alone or together with si-TAB2 (100 nM) or si-con (100 nM) for 24 h followed by 1 μg/ml LPS treatment for 24 h. (A) The protein expression of TAB2 was determined in A549 cells by western blotting. (B) A 3-(4,5-dimethylthiazol-2-yl)-2,5-diphenyltetrazolium bromide assay was performed to detect the viability of A549 cells. (C) The apoptotic rate of A549 cells was examined by flow cytometry. (D-F) Levels of inflammatory-related cytokines in A549 cells were measured by ELISA. *P<0.05. TAB2, TGF-β activated kinase 1 and MAP3K7-binding protein 2; LPS, lipopolysaccharide; miR, microRNA; ALI, acute lung injury; con, control; si-, small interfering RNA; IL, interleukin; TNF-α, tumor necrosis factor α.

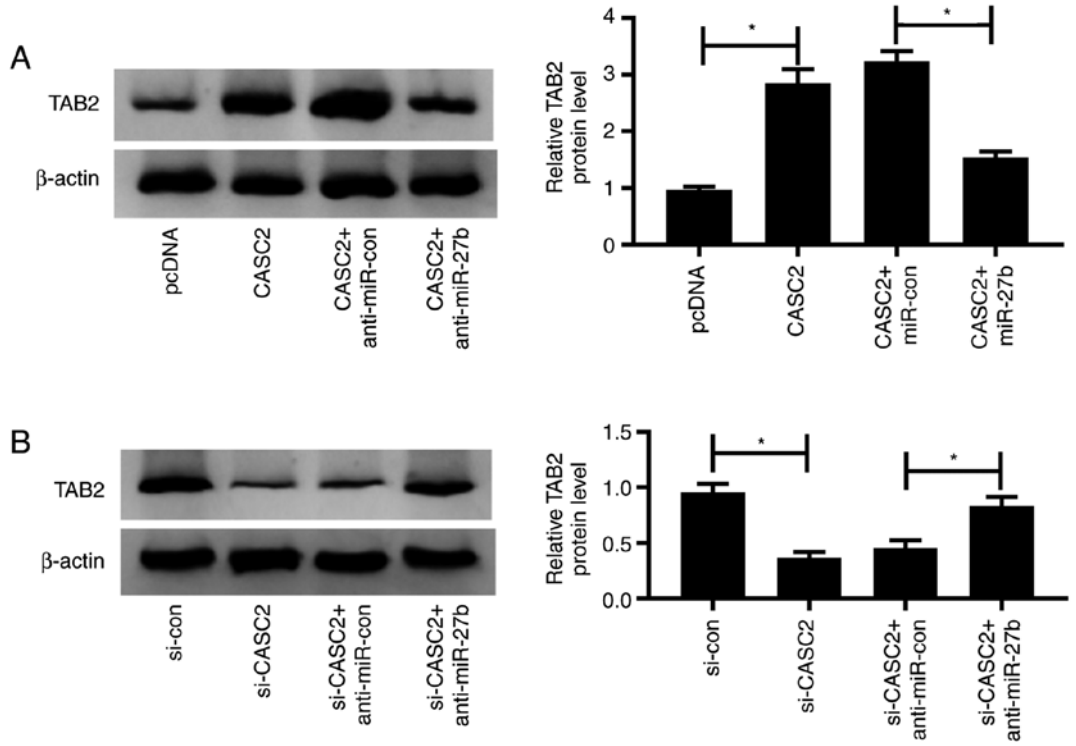

Figure 6. CASC2 upregulates the expression of TAB2 by functioning as a competing endogenous RNA of miR-27b in A549 cells. (A) Western blotting was performed to detect the expression of TAB2 in A549 cells transfected with pcDNA, CASC2, CASC2 + miR-con or CASC2 + miR-27b. (B) A549 cells were transfected with si-con, si-CASC2, si-CASC2 + anti-miR-con or si-CASC2 + anti-miR-27b, and the expression of TAB2 was examined by western blotting. *P<0.05. CASC2, cancer susceptibility candidate 2; TAB2, TGF-β activated kinase 1 and MAP3K7-binding protein 2; miR, microRNA; con, control; si-, small interfering RNA.

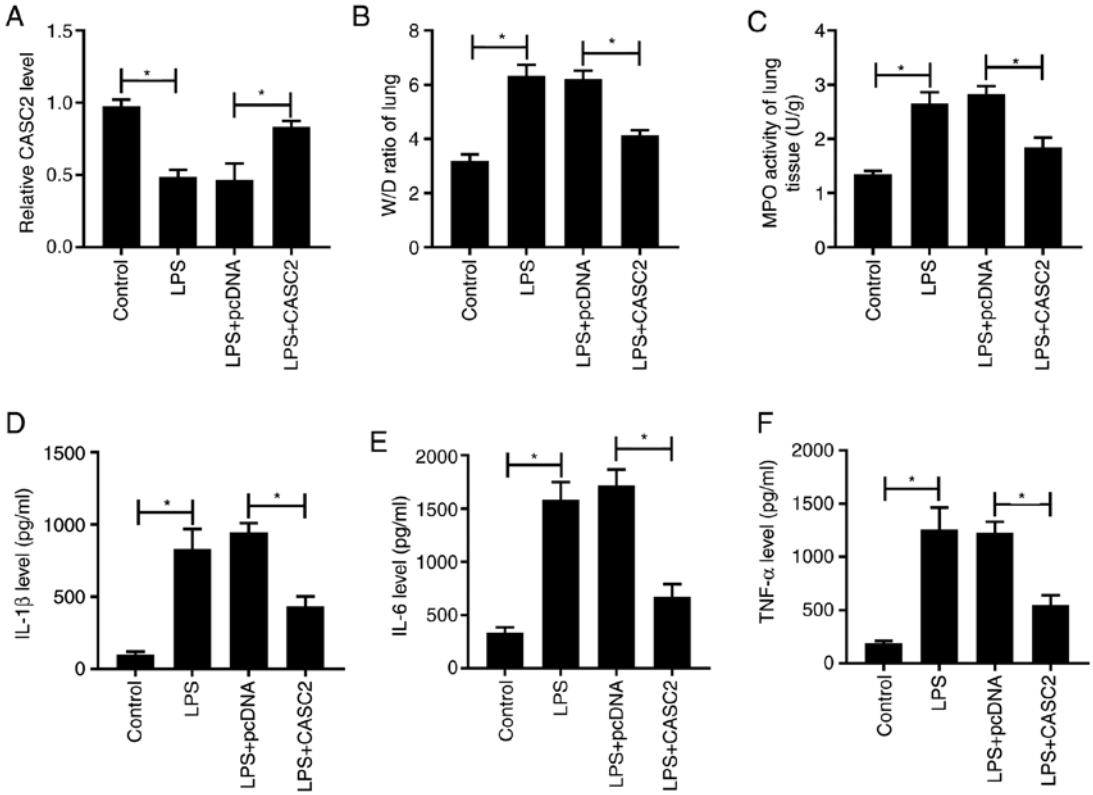

Figure 7. CASC2 overexpression attenuates LPS-induced ALI in lung tissues. (A) Reverse transcription-quantitative PCR was performed to detect the expression of CASC2 in lung tissues in different groups. (B) The W/D ratio of lung tissues was calculated in different groups. (C) The MPO activity of lung tissues was evaluated using an MPO determination kit. (D-F) The inflammatory responses in lung tissues were measured by ELISA. *P<0.05. CASC2, cancer susceptibility candidate 2; LPS, lipopolysaccharide; ALI, acute lung injury; W/D, wet-to-dry; MPO, myeloperoxidase; IL, interleukin; TNF-α, tumor necrosis factor α.

Fig. 7A, LPS treatment decreased the expression of CASC2, whereas overexpression of CASC2 upregulated the expression of CASC2 following LPS treatment. LPS treatment upregulated the W/D ratio, MPO activity and inflammatory factors in lung tissues, these effects were partly reversed by the overexpression of CASC2 (Fig. 7B-F), which suggested that LPS-mediated edema and inflammatory responses were attenuated by the transfection of CASC2. In conclusion, LPS-induced ALI in lung tissues was alleviated by the overexpression of CASC2 *in vivo*.

Discussion

To elucidate the underlying molecular mechanism of LPS-induced ALI, A549 cells were treated with 1 μg/ml LPS for 24 h to construct a cell model of ALI. Cellular inflammatory response was evaluated by measuring the levels of inflammatory markers (IL-1β, IL-6 and TNF-α) via ELISA. Cell viability was reduced, whereas apoptosis and inflammatory responses were increased in the ALI cell model compared with that in the control group. An increasing number of studies have demonstrated that lncRNAs exert important regulatory roles in ALI (21,22). Dai *et al* (23) reported that lncRNA MALAT1 depletion suppressed LPS-induced inflammation via miR-146a. Li *et al* (11) found that lncRNA CASC2 inhibited LPS-induced apoptosis of A549 cells by functioning as a sponge of miR-144-3p. In the present study, it was found that CASC2 overexpression ameliorated LPS-induced injury of A549 cells.

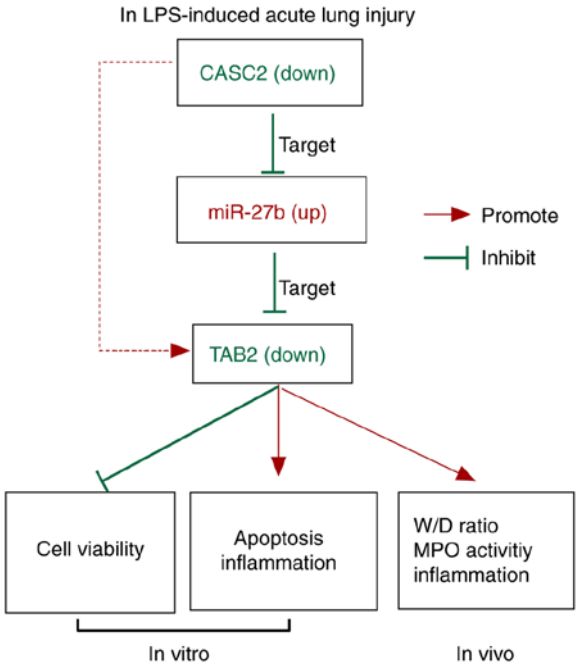

Figure 8. A schema of the working mechanism of CASC2 in acute lung injury. LPS treatment downregulated the expression of CASC2, and the downregulation of CASC2 caused a significant elevation in the expression of miR-27b. miR-27b accumulation downregulated the expression of TAB2. A lower expression of TAB2 was associated with the inhibition of cell viability and the promotion of apoptosis and inflammation. CASC2, cancer susceptibility candidate 2; LPS, lipopolysaccharide; W/D, wet-to-dry; MPO, myeloperoxidase; TAB2, TGF-β activated kinase 1 and MAP3K7-binding protein 2; miR, microRNA.

miR-27b was predicted to directly bind to CASC2 using LncBase database. The binding relationship between miR-27b and CASC2 was validated by dual-luciferase reporter and RIP assays. miR-27b was reported to be involved in the occurrence and development of various types of cancer, including breast cancer and colorectal cancer (24,25). Feng *et al* (26) revealed that miR-27b regulated the metastasis of gastric cancer via nuclear receptor subfamily 2. Wu *et al* (27) reported that lncRNA ZEB2-AS1 accelerated the progression of bladder cancer by targeting miR-27b. However, there are very few studies focused on the role of miR-27b in ALI. Huang *et al* (16) reported that miR-27b facilitated LPS-induced ALI via Nrf2 protein and the NF-κB signaling pathway. In the present study, the expression of miR-27b was higher in the LPS-treated A549 group compared with that in the non-treated group. Additionally, it was found that miR-27b overexpression reversed the protective effects of CASC2 expression on LPS-stimulated A549 cells, and the role of miR-27b in ALI was consistent with the findings of a previous study (16).

miR-27b could modulate the expression of target genes at the posttranscriptional level (25,28,29). In the present study, we hypothesized whether miR-27b regulated the progression of ALI through specific target genes. The complementary sequence between miR-27b and TAB2 3'UTR was predicted using microT-CDS software. Subsequently, the association between miR-27b and TAB2 in A549 cells was validated by conducting dual-luciferase reporter and RIP assays. TAB2 could be downregulated by LPS treatment in A549 cells, and it was demonstrated that TAB2 was negatively regulated by miR-27b in A549 cells. TAB2 is a crucial upstream adaptor of IL-1 signaling. Yang *et al* (17) proposed that miR-142a-3p exerted a protective role in LPS-triggered ALI by downregulating TAB2. Whereas, the present study found that TAB2 exerted the opposite effect in LPS-induced A549 cells compared with the previous study (17). The increased viability and the downregulation of apoptosis and inflammation caused by miR-27b silencing were attenuated by the addition of si-TAB2 in LPS-treated A549 cells. These results demonstrated that miR-27b contributed to LPS-induced ALI via the downregulation of TAB2. The differences in the results with the previous study may be due to the differences in the cells used in the experiment (17). The present study showed that TAB2 was regulated by the CASC2/miR-27b axis, and CASC2 overexpression alleviated LPS-triggered ALI *in vivo*.

There were also some limitations of the present study. Constructing an ALI cell model using two cell lines would make the results more reliable. Furthermore, there was crosstalk within the lncRNAs/miRNAs/mRNAs signal pathway, and additional experiments should be conducted to examine the molecular mechanism of CASC2 in ALI progression.

In summary, miR-27b was found to be a direct target of CASC2, and miR-27b could bind to the 3'UTR of TAB2 in A549 cells. CASC2 protected A549 cells against LPS-induced ALI by upregulating TAB2 via sponging miR-27b (Fig. 8). These results indicated that downregulating the expression of miR-27b could be an effective treatment strategy for patients with ALI.

Acknowledgements

Not applicable.

Funding

No funding was received.

Availability of data and materials

The datasets used and/or analyzed during the current study are available from the corresponding author on reasonable request.

Authors' contributions

XL designed the study. JM, JL and YC performed the experiments. JM and YC analyzed the data. XL wrote the manuscript. All authors read and approved the final manuscript.

Ethics approval and consent to participate

All experimental procedures were approved by The Ethical Committee on Animal Research of Shiyan People's Hospital (Shiyan, China) and were in accordance with guidelines provided by the National Institutes of Health Guide for the Care and Use of Laboratory Animals.

Patient consent for publication

Not applicable.

Competing interests

The authors declare that they have no competing interests.

References

1. Johnson ER and Matthay MA: Acute lung injury: Epidemiology, pathogenesis, and treatment. J Aerosol Med Pulm Drug Deliv 23: 243-252, 2010.
2. Ragaller M and Richter T: Acute lung injury and acute respiratory distress syndrome. J Emerg Trauma Shock 3: 43-51, 2010.
3. Beutler B and Rietschel ET: Innate immune sensing and its roots: The story of endotoxin. Nat Rev Immunol 3: 169-176, 2003.
4. Chow JC, Young DW, Golenbock DT, Christ WJ and Gusovsky F: Toll-like receptor-4 mediates lipopolysaccharide-induced signal transduction. J Biol Chem 274: 10689-10692, 1999.
5. Feng Y, Zou W, Hu C, Li G, Zhou S, He Y, Ma F, Deng C and Sun L: Modulation of CASC2/miR-21/PTEN pathway sensitizes cervical cancer to cisplatin. Arch Biochem Biophys 623-624: 20-30, 2017.
6. Gao Z, Wang H, Li H, Li M, Wang J, Zhang W, Liang X, Su D and Tang J: Long non-coding RNA CASC2 inhibits breast cancer cell growth and metastasis through the regulation of the miR-96-5p/SYVN1 pathway. Int J Oncol 53: 2081-2090, 2018.
7. Li Y, Lv S, Ning H, Li K, Zhou X, Xv H and Wen H: Down-regulation of CASC2 contributes to cisplatin resistance in gastric cancer by sponging miR-19a. Biomed Pharmacother 108: 1775-1782, 2018.
8. Pei Z, Du X, Song Y, Fan L, Li F, Gao Y, Wu R, Chen Y, Li W, Zhou H, *et al*: Down-regulation of lncRNA CASC2 promotes cell proliferation and metastasis of bladder cancer by activation of the Wnt/β-catenin signaling pathway. Oncotarget 8: 18145-18153, 2017.
9. Wang Y, Liu Z, Yao B, Li Q, Wang L, Wang C, Dou C, Xu M, Liu Q and Tu K: Long non-coding RNA CASC2 suppresses epithelial-mesenchymal transition of hepatocellular carcinoma cells through CASC2/miR-367/FBXW7 axis. Mol Cancer 16: 123, 2017.
10. Ba Z, Gu L, Hao S, Wang X, Cheng Z and Nie G: Downregulation of lncRNA CASC2 facilitates osteosarcoma growth and invasion through miR-181a. Cell Prolif 51: e12409, 2018.

11. Li H, Shi H, Gao M, Ma N and Sun R: Long non-coding RNA CASC2 improved acute lung injury by regulating miR-144-3p/AQP1 axis to reduce lung epithelial cell apoptosis. Cell Biosci 8: 15, 2018.
12. Lu J, Getz G, Miska EA, Alvarez-Saavedra E, Lamb J, Peck D, Sweet-Cordero A, Ebert BL, Mak RH, Ferrando AA, *et al*: MicroRNA expression profiles classify human cancers. Nature 435: 834-838, 2005.
13. Hammond SM: An overview of microRNAs. Adv Drug Deliv Rev 87: 3-14, 2015.
14. Sand M: The pathway of miRNA maturation. Methods Mol Biol 1095: 3-10, 2014.
15. Li W, Ma K, Zhang S, Zhang H, Liu J, Wang X and Li S: Pulmonary microRNA expression profiling in an immature piglet model of cardiopulmonary bypass-induced acute lung injury. Artif Organs 39: 327-335, 2015.
16. Huang Y, Huang L, Zhu G, Pei Z and Zhang W: Downregulated microRNA-27b attenuates lipopolysaccharide-induced acute lung injury via activation of NF-E2-related factor 2 and inhibition of nuclear factor κB signaling pathway. J Cell Physiol 234: 6023-6032, 2019.
17. Yang Y, Yang C, Guo YF, Liu P, Guo S, Yang J, Zahoor A, Shaukat A and Deng G: MiR-142a-3p alleviates Escherichia coli derived lipopolysaccharide-induced acute lung injury by targeting TAB2. Microb Pathog 136: 103721, 2019.
18. Chuang CY, Chen TL, Cherng YG, Tai YT, Chen TG and Chen RM: Lipopolysaccharide induces apoptotic insults to human alveolar epithelial A549 cells through reactive oxygen species-mediated activation of an intrinsic mitochondrion-dependent pathway. Arch Toxicol 85: 209-218, 2011.
19. Livak KJ and Schmittgen TD: Analysis of relative gene expression data using real-time quantitative PCR and the 2(-Delta Delta C(T)) method. Methods 25: 402-408, 2001.
20. National Research Council Institute for Laboratory Animal R. In: Guide for the Care and Use of Laboratory Animals. Washington (DC): National Academies Press (US) Copyright 1996 by the National Academy of Sciences. All rights reserved, 1996.
21. Li H, Shi H, Ma N, Zi P, Liu Q and Sun R: BML-111 alleviates acute lung injury through regulating the expression of lncRNA MALAT1. Arch Biochem Biophys 649: 15-21, 2018.
22. Liu G, Mei H, Chen M, Qin S, Li K, Zhang W and Chen T: Protective effect of agmatine against hyperoxia-induced acute lung injury via regulating lncRNA gadd7. Biochem Biophys Res Commun 516: 68-74, 2019.
23. Dai L, Zhang G, Cheng Z, Wang X, Jia L, Jing X, Wang H, Zhang R, Liu M, Jiang T, *et al*: Knockdown of LncRNA MALAT1 contributes to the suppression of inflammatory responses by up-regulating miR-146a in LPS-induced acute lung injury. Connect Tissue Res 59: 581-592, 2018.
24. Chen D, Si W, Shen J, Du C, Lou W, Bao C, Zheng H, Pan J, Zhong G, Xu L, *et al*: miR-27b-3p inhibits proliferation and potentially reverses multi-chemoresistance by targeting CBLB/GRB2 in breast cancer cells. Cell Death Dis 9: 188, 2018.
25. Luo Y, Yu SY, Chen JJ, Qin J, Qiu YE, Zhong M and Chen M: MiR-27b directly targets Rab3D to inhibit the malignant phenotype in colorectal cancer. Oncotarget 9: 3830-3841, 2018.
26. Feng Q, Wu X, Li F, Ning B, Lu X, Zhang Y, Pan Y and Guan W: miR-27b inhibits gastric cancer metastasis by targeting NR2F2. Protein Cell 8: 114-122, 2017.
27. Wu X, Yan T, Wang Z, Wu X, Cao G and Zhang C: LncRNA ZEB2-AS1 promotes bladder cancer cell proliferation and inhibits apoptosis by regulating miR-27b. Biomed Pharmacother 96: 299-304, 2017.
28. Ling YH, Sui MH, Zheng Q, Wang KY, Wu H, Li WY, Liu Y, Chu MX, Fang FG and Xu LN: miR-27b regulates myogenic proliferation and differentiation by targeting Pax3 in goat. Sci Rep 8: 3909, 2018.
29. Rong X, Ge D, Shen D, Chen X, Wang X, Zhang L, Jia C, Zeng J, He Y, Qiu H, *et al*: miR-27b suppresses endothelial cell proliferation and migration by targeting Smad7 in kawasaki disease. Cell Physiol Biochem 48: 1804-1814, 2018.